Nov 6th, 12:00 AM - 12:00 AM

Direct Strength Method for Ultimate Strength of Bolted Moment-Connections between Cold-Formed Steel Channel Members

James B. P. Lim

Gregory J. Hancock

G. Charles Clifton

Cao Hung Pham

Twenty-Second International Specialty Conference on Cold-Formed Steel Structures
St. Louis, Missouri, USA, November 5 & 6, 2014

Direct Strength Method for Ultimate Strength of Bolted Moment-Connections between Cold-Formed Steel Channel Members

James B.P. Lim[1], Gregory J. Hancock[2], G. Charles Clifton[3], Cao Hung Pham[4]

Abstract

Experimental tests have previously shown that the strength of bolted moment-connections between cold-formed steel members, where the connections are formed through an array of bolts in the web, is dependent on the length of the bolt-group. This reduced strength has been observed in tests on portal frame joints as well as over-lapped purlin joints. For a short bolt-group length, in the order of the depth of the section, this paper shows that a reasonable lower bound to this reduced strength can be predicted by using the Direct Strength Method (DSM), modified to include the effect of the bimoment at the connection. The upper bound would be the full in-plane major axis moment-capacity of the section, which can be achieved with a long bolt-group length and can also be predicted using the conventional DSM.

---

[1] Senior Lecturer, Department of Civil and Environmental Engineering, The University of Auckland, New Zealand.
[2] Emeritus Professor, School of Civil Engineering, The University of Sydney, Sydney NSW 2006, Australia.
3 Associate Professor, Department of Civil and Environmental Engineering, The University of Auckland, New Zealand.
[4] ARC Postdoctoral Fellow, School of Civil Engineering, The University of Sydney, Sydney NSW 2006, Australia.

Introduction

Baigent and Hancock (1982) have previously described full-scale portal frame tests in which single cold-formed steel channel-sections were used for the column and rafter members. The joints of the frame tested were rigid. Failure was observed at a strength less than that of the in-plane major axis moment capacity of the channel-sections, which was explained as being due to the presence of a bimoment (Vlasov (1961), Zbirohowski-Koscia (1967)) (resulting from the eccentricity of the major axis moment generated in the web of the channel section by the bolt-group from the shear center of the channel-section). The bimoment B is equal to the product of the major axis moment, $M^*_{x,}$ and eccentricity of the web centreline from the shear center. Further detail is given in Hancock (1985). The stress distribution of this combined effect is shown in Fig. 1.

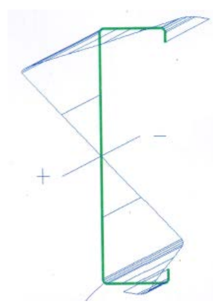

Figure 1: Stress distribution due to combined bending and bimoment (compression is –ve and tension is +ve)

The bimoment, generated by the eccentricity as described above, puts each flange into bending about its own (horizontal) plane. For a channel subject to negative major axis moment (i.e. bottom flange in compression), the bimoment generates compression stress at the bottom flange/web junction, which adds to the major axis bending-induced compression stress, while at the bottom flange/lip junction the bimoment generates tensile stress, which opposes the major axis bending induced compression stress. The result is increased compression stress in the bottom half of the web and the inside part of the bottom flange, but with the outside part of the bottom flange in tension as shown in Fig 1. This effectively anchors the bottom flange against distortional buckling, but reduces the local buckling critical stress in the web.

Lim and Nethercot (2004) have also conducted full-scale cold-formed steel portal frame tests. Fig. 2 shows a photograph of the test conducted. As can be seen, the test was conducted horizontally on the laboratory floor. Lateral restraints were applied to the web of the channel-sections, away from the flanges eliminating lateral-torsional buckling.

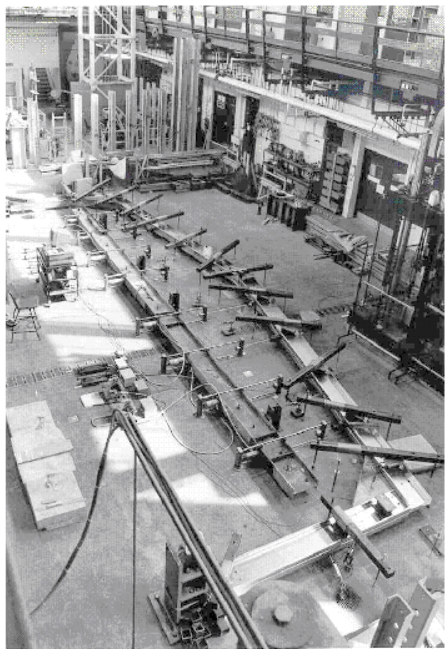

Figure 2: Full-scale portal frame test after Lim and Nethercot [2]

Unlike the portal frames tested by Baigent and Hancock, where single channel-sections were used, Lim and Nethercot used back-to-back channel-sections. Furthermore, the joints of the portal frame tested by Lim and Nethercot were formed through brackets, bolted through the webs of channel-sections being connected. Details of the apex joint are shown in Fig. 3; a similar arrangement was used for the eaves joint. Also, unlike the joints of Baigent and Hancock which were rigid, formed through rigid cover plates and friction grip bolts, the joints tested by Lim and Nethercot were semi-rigid, which could be attributed principally to the effects of bolt-hole elongation.

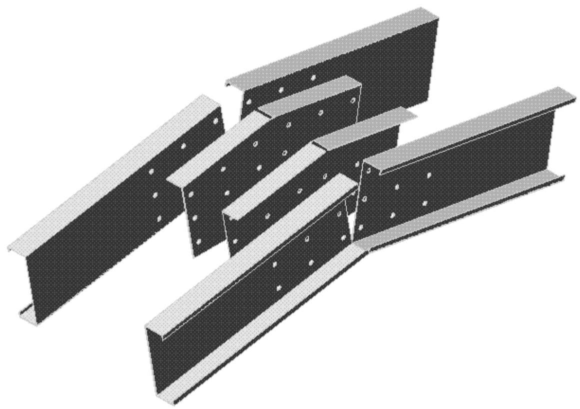

Figure 3: Details of apex joint after Lim and Nethercot [2]

Lim and Nethercot tested two frames, to be referred to as Frames A and B. Both frames were of span 12 m and height 3 m. The difference between the two frames was the size of the joints, which were based around two different bolt-group sizes (a_B x b_B) for the joints of 315 mm x 230 mm and 615 mm x 230 mm for Frames A and B, respectively. It was observed from the frame tests that Frame A, having the shorter bolt-group length, failed at a load approximately 20% lower than that of Frame B, having the longer bolt-group length.

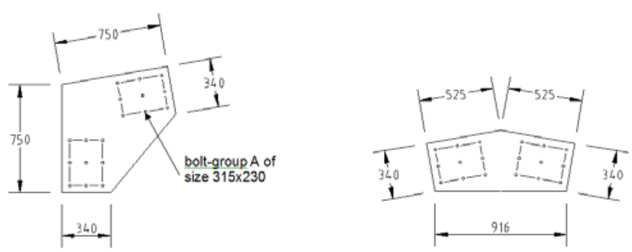

(a) Joints of Frame A

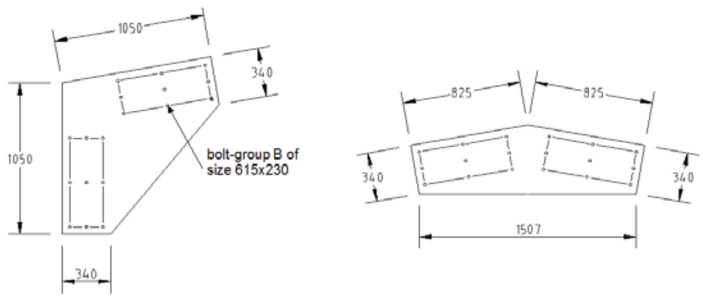

(b) Joints of Frame B

Figure 4: Details of bolt-groups and corresponding sizes of eaves and apex brackets

This paper proposes that the difference in the moment carrying capacity of Frame A and B can still be attributed to the bimoment, even though back-to-back channel-sections were used. It is argued that the channel-sections should still be considered to act independently with respect to the bimoment, and that the bimoment should not be ignored because back-to-back channel-sections were used. Figure 5 shows the separated channel-sections taken from the joints after failure. For the shorter bolt-group the failure mode from this combined action of in-plane moment and bimoment is shown in Fig 5(a). The bucking induced by compression is in the bottom half of the web and in the flange/lip region of the opposite flange. For the longer bolt-group the failure mode is distortional buckling, with the flange/lip intersection buckling, interacting with local buckling as the elastic critical buckling stress of both modes is very similar. This is shown in Fig 5(b).

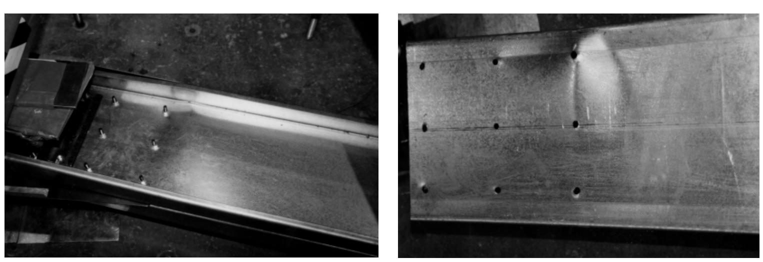

(a) Shorter bolt-group

(b) Longer bolt-group

Figure 5: Separated channel-sections

The bimoment explanation of Baigent and Hancock assumes an applied moment in the web. As shown in Figure 6(a), it can come from a bolt group, or, in the Baigent and Hancock case, from a plate clamped onto the web alone. It can therefore be seen to be applicable to a back-to-back channel section configuration and is used to explain the reduced moment-capacity of the channel-section for short bolt-group sizes. For long bolt-groups, the bending moment to be sustained by the channel-sections is transferred through a couple in the web, the large forces of which are perpendicular to the axis of the web, as shown in Figure 6(b), and are applied away from the shear center. The forces leading to the couple in the web are smaller, and so by St Venant's theory, Engineering Bending Theory (EBT) is more likely to hold at the end of the bolt-group, and consequently the effects of the bimoment are no longer as significant. This explains why the strength is reduced for a smaller bolt-group size and not for a larger bolt-group size where the EBT stresses are mobilised in the section.

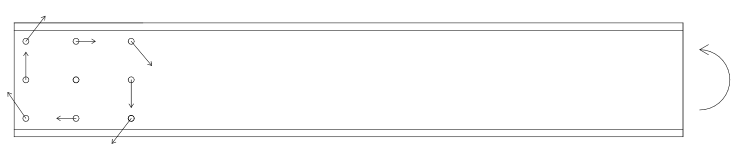

(a) Free body diagram of short bolt-group when joint is in pure bending

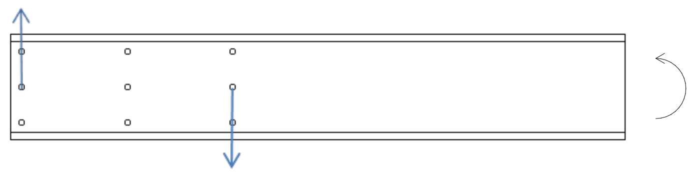

(b) Vertical component of forces in bolt-group generated by a long bolt-group

Figure 6 Couples for short and long bolt-groups

In this paper, the Direct Strength Method (DSM) of design as specified in Section 7 of AS/NZS 4600:2005 and Appendix 1 of the North American Specification NAS S100:2012 is used to provide an estimate of the moment capacity for such joints. The results are compared with the experimental results of Lim and Nethercot.

Experimental tests

Four apex joints were tested by Lim and Nethercot (2003) under pure bending. For completeness, these tests are briefly described in this Section.

Fig. 7 shows the parameters used to define the geometry of the back-to-back apex brackets used in each test. The lip stiffener along the compression edge of the apex brackets prevents buckling of the free-edge. In all four tests, no buckling of the apex brackets was observed.

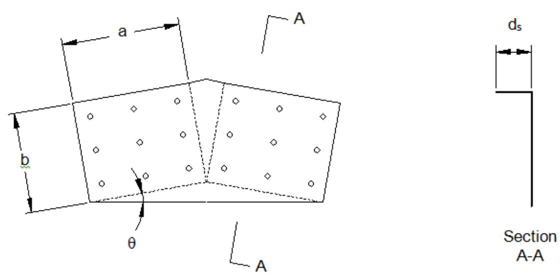

Figure 7: Diagram showing parameters of apex bracket

The dimensions of the apex bracket used for each joint are summarised in Table 1. Each joint used a different length of bolt-group (and therefore a different size of apex bracket); all bolt-groups were formed from an array of nine bolts. The nominal thickness of each bracket was 4 mm and the nominal diameters of the bolts and bolt-holes were 16 mm and 18 mm, respectively. The average yield and ultimate strengths of the brackets, measured from three tensile coupons taken from each bracket, were 341 N/mm^2 and 511 N/mm^2, respectively.

Table 1: Dimension of apex brackets tested

	Bracket			Bolt-group	
Test	a (mm)	b (mm)	t (mm)	a_B (mm)	b_B (mm)
1	525	340	3.98	315	230
2	600	340	3.98	390	230
3	675	340	3.98	465	230
4	825	340	3.98	615	230

The average dimensions of the channel-sections used in the tests are shown in Fig.8. The average yield and ultimate strengths were determined from tensile testing to be 358 N/mm^2 and 425 N/mm^2, respectively.

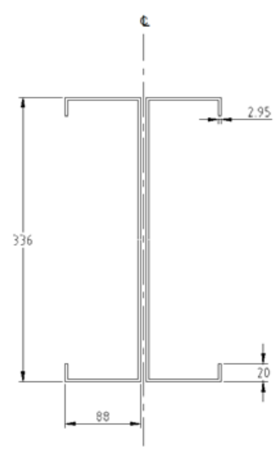

Figure 8: Average dimensions of back-to-back channel-sections used in apex joint tests

A photograph of the laboratory test arrangement is shown in Fig.9. The apex joint was tested horizontally on the laboratory floor. The apex joint was loaded under pure bending.

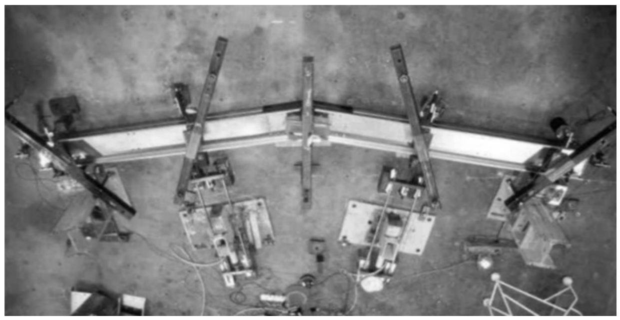

Figure 9: Photograph of the laboratory test set-up of apex joint

Table 2 shows the ratio a_B/D and the ultimate moment M_u^{exp} for all four apex joints.

Table 2: Experimental test results

Test	a_B (mm)	a_B/D	M_u^{exp} (kN.m)
1	315	0.94	75.0
2	390	1.16	77.5
3	465	1.38	82.5
4	615	1.83	87.5

It can be seen from Table 2 that as the value of a_B/D increases, the ultimate moment also increases. For example, Test 1, having a ratio of a_B/D of 0.93, failed at a bending moment 23% less than the moment capacity of the back-to-back channel-section. On the other hand, Test 4, having a ratio of a_B/D of 1.81, failed at a bending moment only 10% less than the moment capacity of the back-to-back channel-sections.

Application to Direct Strength Method (DSM)

In Section 7 of AS/NZS 4600:2005 [Appendix 1 of NAS(2007)], the nominal member moment capacity (M_b) is the least of the nominal member moment capacity (M_{be}) for lateral-torsional buckling, the nominal member moment capacity (M_{bl}) for local buckling, and the nominal member moment capacity (M_{bd}) for distortional buckling.

The nominal member moment capacity at local buckling *(M_{bl})* is determined from Section 7.2.2.3 of AS/NZS 4600:2005 [Appendix 1, Section 1.2.2.2 of NAS (2007)] as follows:

For $\lambda_l \leq 0.776$: $M_{bl} = M_{be}$ (1)

For $\lambda_l > 0.776$: $M_{bl} = \left[1 - 0.15\left(\frac{M_{ol}}{M_{be}}\right)^{0.5}\right]\left(\frac{M_{ol}}{M_{be}}\right)^{0.5} M_{be}$ (2)

where λ_l is non-dimensional slenderness used to determine M_{bl} ; $\lambda_l = \sqrt{M_{be} / M_{ol}}$

M_{ol} is the elastic local buckling moment of the section; $M_{ol} = Z_f f_{ol}$ where Z_f is the section modulus about a horizontal axis of the full section, f_{ol} is the elastic local buckling stress of the section in bending and M_{be} is the nominal member moment capacity for lateral-torsional buckling of the full section.

For the tests in this paper, lateral-torsional buckling has been prevented by lateral braces so that $M_{be} = M_y$ in Eq. 2 where $M_y = Z_f f_y$. Consequently, M_{bl} becomes the local buckling section moment capacity M_{sl}.

The nominal member moment capacity at distortional buckling *(M_{bd})* is determined from Section 7.2.2.4 of AS/NZS 4600:2005 [Appendix 1, Section 1.2.2.3 of NAS (2007)] as follows:

For $\lambda_d \leq 0.673$: $M_{bd} = M_y$ (3)

For $\lambda_d > 0.673$: $M_{bd} = \left[1 - 0.22\left(\frac{M_{od}}{M_y}\right)^{0.5}\right]\left(\frac{M_{od}}{M_y}\right)^{0.5} M_y$ (4)

where λ_d is non-dimensional slenderness used to determine M_{bd} ; $\lambda_d = \sqrt{M_y / M_{od}}$, f_{od} is the elastic distortional buckling moment of the section;

$M_{od} = Z_f f_{od}$ where f_{od} is the elastic distortional buckling stress of the section in bending.

For the purpose of the notation used in this paper, the section nominal distortional moment capacity M_{sd} is put equal to M_{bd}.

The computer program THIN-WALL (CASE (2006)) has been used to compute the signature curve for the section subject to pure bending as shown in Fig. 10(a) where the local buckling stress is f_{ol} = 450.1 N/mm^2 and distortional buckling stress f_{od} = 369.2 N/mm^2. For the section subject to bending plus bimoment, the signature curve is shown in Fig. 10(b), where the local buckling stress is f_{ol} = 448.4 N/mm^2. However, the distortional buckling minimum no longer exists due to the tension at the lips caused by the bimoment. The local buckling stress is very similar to that in Fig 10(a) probably because the local buckling is mainly in the web as shown in Fig. 11.

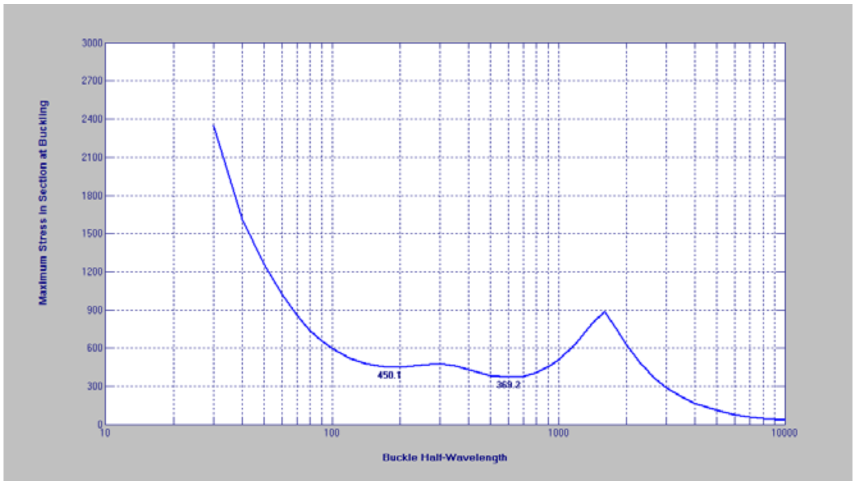

(a) Pure bending

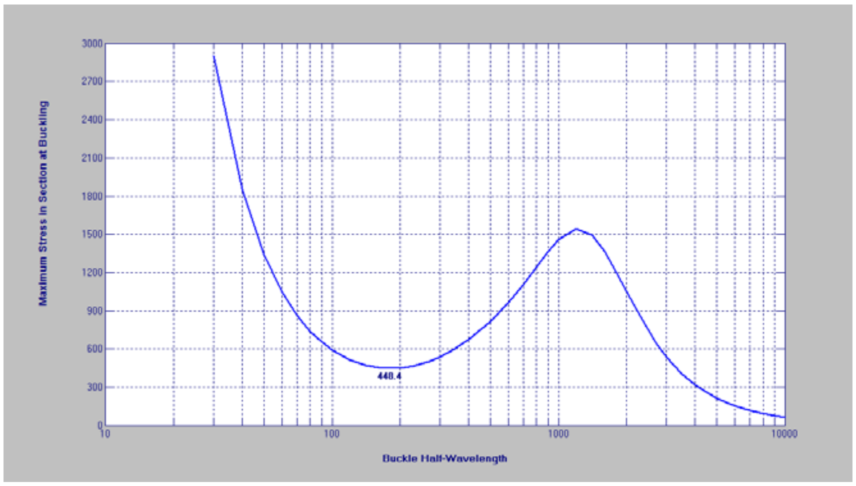

(b) Bending plus bimoment

Figure 10: Signature curves for test channel section

Using the dimensions of the channel-section, the moment-capacity of the back-to-back channel sections M_{sl} is calculated using Equation 2 to be 97.5 kN.m for two sections and M_{sd} using Equation 4 is calculated to be 83.94 kN.m. These can be compared to 96.8 kN.m, calculated in accordance with the British Standard (BS5950: Part 5 (1998)), which it should be noted does not take into account distortional buckling. It is interesting to observe that the distortional buckling section moment capacity M_{sd} is slightly below (4%) the experimental test result for Test 4 of 87.5 kN.m given in Table 2 for the long bolt-group case. In the case of the long bolt-group, distortional buckling occurs as shown in Figure 5 (b) since the whole flange is most likely in uniform compression as assumed for the signature curve in Fig. 10(a). The slightly higher experimental result (87.5 kN.m cf 83.94 kN.m) may be a result of the fact that pure bending has not been fully mobilised even for the longer bolt-group.

For the case of bending plus bimoment, the applied moment at buckling is computed from the THIN-WALL analysis to be M_{ol2} = 69.54 kN.m for the two channels. Using the dimensions of the channel-section, the moment-capacity of the back-to-back channel sections, M_{sl2} is calculated using Equation 2 to be 78.44 kN.m for two sections. This compares well with 75.0 kN.m for Test 1 where a short bolt-group has been used.

Figure 11 shows the buckled shape for the case of major axis bending plus bimoment. As can be seen, there is no displacement of the flange/lip junction, and is consistent with the deformed shape of Fig. 5(a) pertaining to the shorter bolt-group.

Figure 11: Buckling mode for bending and bimoment (compression at bottom)

Comparison against tests of Wong and Chung (2002)

Wong and Chung (2002) have also reported tests on beam-to-column joints of a cold-formed steel multi-storey frame. It should be noted that the test arrangement adopted in their test arrangements induced some shear at the joints. Two sections were considered:

- C15016DS: Section depth of 152 mm, thickness of 1.6 mm
- C15020DS: Section depth of 152 mm and thickness of 2.0 mm

The experimentally determined moment capacity of the C15016DS and C15020DS sections in pure bending is 16.95 kN.m and 21.36 kN.m, respectively. The C15016DS is more slender and the DSM using M_{sl2} equal to 15.14 kN.m as described above predicts the mean failure moment of 14.82 kN.m well with a ratio of joint test moment/DSM theory of 0.98. The C12020DS is unconservatively predicted by the DSM using M_{sl2} equal to 21.33 kN.m as described above with a ratio of joint test moment/DSM theory of 0.91 for a test moment of 19.5 kN.m. The explanation is that the C12020DS Section is quite stocky so yielding and distortional buckling rather than local buckling probably control. Note that in Fig 4 of the Wong and Chung paper that the failure mode is across the whole flange and contains an element of distortional buckling. It is also interesting to note that a prediction based on M_{sd} equal to 21.20 kN.m from Equation 4 gives a ratio of pure bending test moment/DSM theory for this section of 1.01. This section is similar to the Baigent and Hancock frame section where yielding controlled at the joint, rather than inelastic local buckling (note that M_{ol} = 49.52 kN.m cf M_y = 25.0 kN.m for two sections). A model based on first yield (M_{y2}) at the flange/web junction due to the major axis moment and bimoment as a criterion is very conservative with M_{y2} = 11.95 kN.m << Test moment = 19.5 kN.m. Baigent and Hancock used an inelastic model with yielding lowering the signature curve to get a good estimate.

Conclusions

Based on the limited test results available, the DSM model using M_{sl2} for the short bolt-group can be seen to be reasonable for slender sections where local buckling with some yielding controls. The DSM model using M_{sd} for the long bolt-group can be seen to be reasonable for the slender sections. For stockier sections, a partial yielding model is needed. The DSM model does not predict the partial yielding due to the bimoment and assumes that M_y is for the full section yielding; only M_{ol2} takes into account the bimoment. Further work is required, but the results so far appear consistent with those of Baigent and Hancock (1982).

References

American Iron and Steel Institute (AISI) (2007). "North American Specification for the Design of Cold-Formed Steel Structural Members." 2007 Edition, AISI S100-2007.

Baigent, A. H. and Hancock, G. J. (1982). The strength of cold-formed portal frame. *Recent Research and Development in Cold-Formed Steel Design and Construction, St. Louis, University of Missouri-Rolla*, pp.321-347.

BS5950: Part 5 (1998). *Code of practice for design of cold-formed sections*, London, British Standards Institution.

CASE. (2006). "THIN-WALL – A Computer Program for Cross-Section Analysis and Finite Strip Buckling Analysis and Direct Strength Design of Thin-Walled Structures." Version 2.1, Centre for Advanced Structural Engineering, School of Civil Engineering, The University of Sydney.

Hancock, G.J. (1985). Portal frames composed of cold-formed channel sections, Chapter 8, Steel Framed Structures, Ed. R. Narayanan, Elsevier Applied Science Publishers, London.

Lim, J.B.P. and Nethercot, D.A. (2004). Finite element idealisation of a cold-formed steel portal frame. *Journal of Structural Engineering*, ASCE, 130 (1), pp. 78-94.

Lim, J.B.P. and Nethercot, D.A. (2003). Ultimate strength of bolted moment connections between cold-formed steel members. *Thin-Walled Structures*, 41(11), pp. 1019.

Standards Australia. (2005). "AS/NZS 4600:2005, Cold-Formed Steel Structures." Standards Australia/ Standards New Zealand.

Vlasov, V.Z. (1961). Thin-Walled Elastic Beams, Israel Program for scientific Translation, Jerusalem, 1961.

Wong, M.F. and Chung, K.F. (2002). Structural behaviour of bolted moment connections in cold-formed steel beam-column sub-frames, *Jour. Constr. Steel Res*., 58, No. 2, p253.

Zbirohowski-Koscia, K. (1967). Thin-Walled Beams – From Theory to Practice, Crosby Lockwood, London.